

Accepted Manuscript

Synthesis, Structural, Continuous shape measure and Bond valence sum characterization of bismuth(III) complexes of substituted dithiocarbamates and their solvothermal decomposition

Subbarayan Sivasekar, Kuppukkannu Ramalingam, Corrado Rizzoli, Nagarajan Alexander

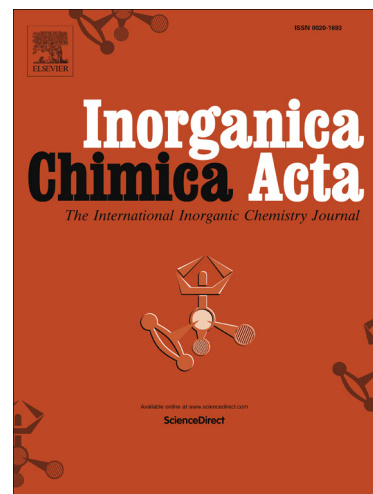
PII: S0020-1693(14)00283-7
DOI: <http://dx.doi.org/10.1016/j.ica.2014.04.042>
Reference: ICA 15990

To appear in: *Inorganica Chimica Acta*

Received Date: 11 January 2014
Revised Date: 23 April 2014
Accepted Date: 28 April 2014

Please cite this article as: S. Sivasekar, K. Ramalingam, C. Rizzoli, N. Alexander, Synthesis, Structural, Continuous shape measure and Bond valence sum characterization of bismuth(III) complexes of substituted dithiocarbamates and their solvothermal decomposition, *Inorganica Chimica Acta* (2014), doi: <http://dx.doi.org/10.1016/j.ica.2014.04.042>

This is a PDF file of an unedited manuscript that has been accepted for publication. As a service to our customers we are providing this early version of the manuscript. The manuscript will undergo copyediting, typesetting, and review of the resulting proof before it is published in its final form. Please note that during the production process errors may be discovered which could affect the content, and all legal disclaimers that apply to the journal pertain.



1 **Synthesis, Structural, Continuous shape measure and Bond valence sum**
2 **characterization of bismuth(III) complexes of substituted dithiocarbamates and their**
3 **solvothermal decomposition**

4 **Subbarayan Sivasekar,^a Kuppukkannu Ramalingam,^{* a} Corrado Rizzoli^b and**
5 **Nagarajan Alexander^a**

6 ^a*Department of Chemistry, Annamalai University, Annamalainagar 608 002, India*

7 ^b*Department of General and Inorganic Chemistry, University of Parma, Parma-43100, Italy*

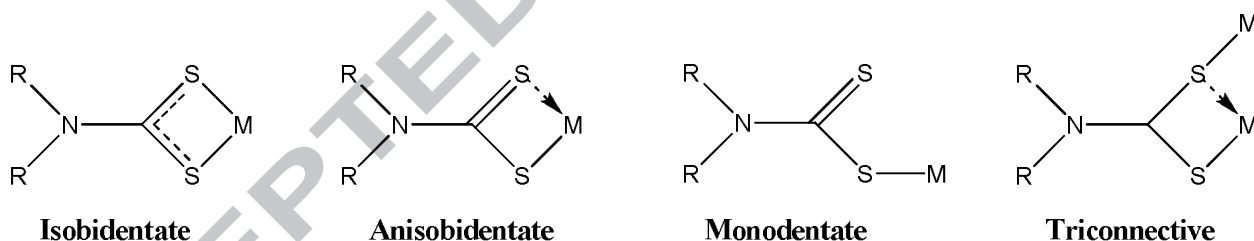
8
9 Bismuth(III) complexes, [Bi(chmdtc)₃] (**1**) [Bi(chedtc)₃] (**2**) and [Bi(dchdte)₃] (**3**), (where
10 chmdtc = cyclohexylmethyldithiocarbamate, chedtc = cyclohexylethyldithiocarbamate and dchdte =
11 dicyclohexyldithiocarbamate) have been prepared and characterized by electronic, IR, NMR (¹H
12 and ¹³C) spectra, and single crystal X-ray diffraction. Electronic spectra of the complexes show
13 signature bands in the range: 418-423 nm due to charge transfer transitions. The characteristic
14 thioureide bands occur at 1474, 1467 and 1443 cm⁻¹ for (**1**), (**2**) and (**3**) respectively. Single crystal
15 X-ray structures of [Bi(chmdtc)₃] (**1**), [Bi(chedtc)₃] (**2**) and [Bi(dchdte)₃] (**3**) indicate that the short
16 Bi---S interactions between the molecules lead to dimeric structures. CShM calculations on the
17 chromophores clearly quantify the extent of deviation from the ideal geometry. BiS₆ chromophore
18 in (**1**) is a distorted octahedron. The coordination geometry for both [Bi(chedtc)₃] (**2**) and
19 [Bi(dchdte)₃] (**3**) should be better described as distorted pentagonal pyramidal. The higher BVS
20 values observed in the present set of compounds support the fact that the Bi-S bonds are more
21 covalent.

* Corresponding author, Tel.:+91 413 2202834; fax: +91 414 422265.
E-mail address: krauchem@yahoo.com (K. Ramalingam)

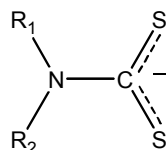
22 **Keywords:** Bismuth(III); dithiocarbamate; non-covalent interactions; pentagonal pyramid; crystal
 23 structures; nanosulfide.

24 1. Introduction

25 Bismuth is a group 15 element with the most common formal oxidation state of +3. Bismuth
 26 compounds have long been used as therapeutic agents. The chalcogenides of bismuth(III) find
 27 increasing applications in solar cells, photolithography, optical memory devices and as photo- and
 28 thermo-electric conductors [1,2]. Trivalent bismuth xanthates, dithiocarbamates and alkyl- as well
 29 as alkylenedithiophosphates have been prepared and some of the dithio derivatives show interesting
 30 catalytic and biocidal applications [3,4]. The antimicrobial and anti-tumor activity of binary
 31 bismuth(III) dithiocarbamates of the general formula, $\text{Bi}(\text{S}_2\text{CNR}_2)_3$ has been reported [5].
 32 Dithiocarbamates are known to show a variety of coordination modes such as isobidentate,
 33 anisobidentate, monodentate and triconnective [6]. Bismuth dithiocarbamates serve as useful



35
 36 precursors for the preparation of Bi_2S_3 and offer a facile transformation at low temperature
 37 compared to the traditional high sintering temperature methods [7-11]. In continuation of our efforts
 38 to identify new precursors for the preparation of Bi_2S_3 , we report the synthesis and characterization
 39 of $[\text{Bi}(\text{chmdtc})_3]$ (**1**), $[\text{Bi}(\text{chedtc})_3]$ (**2**) and $[\text{Bi}(\text{dchdtc})_3]$ (**3**). On heating the trisdithiocarbamates in
 40 diethylenetriamine, in a non-conventional solvothermal process, *nano* Bi_2S_3 separated which was
 41 characterized by SEM, EDS and HRTEM techniques.



Cyclohexylmethyldithiocarbamate
(chmdtc)

$R_1: -CH_3, R_2: -C_6H_{11}$

Cyclohexylethyldithiocarbamate
(chedtc)

$R_1: -C_2H_5, R_2: -C_6H_{11}$

Dicyclohexyldithiocarbamate
(dchdtc)

$R_1, R_2: -C_6H_{11}$

42
43

44 2. Experimental

45 Bismuth nitrate (SD fine chemicals, India), the parent amines (Fisher Scientific, India) and
46 the solvents (SD fine chemicals, India) were commercially available analytical grade materials and
47 were used as supplied without further purification. Melting points of solid products were
48 determined with digital melting / boiling point apparatus, Jains, India. Elemental analyses were
49 carried out with Elementar, Vario Micro Cube instrument. IR spectra were recorded on an Avatar
50 Nicolet FT-IR spectrometer (range 4000–400 cm^{-1}) as KBr pellets of the compounds. Electronic
51 spectra were recorded in CCl_4 on a Hitachi U-2001 double beam spectrometer. Thermal analysis
52 was carried out with NETZSCH STA 449F3 instrument under nitrogen atmosphere with a heating
53 rate of 10 K / minute. 1H and ^{13}C NMR spectra were recorded on a Bruker AMX-400 spectrometer
54 at room temperature using $CDCl_3$ as solvent. NMR spectra were recorded at room temperature with
55 TMS as an internal reference and $CDCl_3$ as the solvent. The powder diffraction data were collected
56 in the 2θ range = 2-80° using Bruker-D8 X-ray diffractometer equipped with Cu- $K\alpha$ radiation at
57 fixed current and potential. The scan speed and step sizes were 0.05 ° min^{-1} and 0.00657
58 respectively. Scanning electron micrographs of the samples were recorded with JEOL JSM-
59 5610Lv microscope. HRTEM measurements were carried out on JEOL 2100 (Field emission)
60 with an accelerating voltage of 200kV. Some important infra red spectral bands and the

61 electronic spectral data are listed in Table 1. NMR spectral data of bismuth complexes are listed in
62 Table 2.

63 2.1 X-ray crystallography

64 Intensity data were collected at ambient temperature (295 K) on a Bruker APEX-II CCD
65 diffractometer with graphite monochromated MoK α radiation ($\lambda = 0.71073 \text{ \AA}$) and were corrected
66 for absorptions with a multi-scan technique [12-14]. The structures were solved by direct methods
67 using SIR97 and were refined by SHELX97 [15]. The non-hydrogen atoms were refined
68 anisotropically and all the hydrogen atoms were fixed geometrically. Molecular plots were obtained
69 using the ORTEP-3 program [16]. In (2), the CCl₄ solvent molecule and one cyclohexyl group are
70 disordered over two sets of orientations with site occupancy of 0.5. One ethyl group is also
71 disordered over two orientations with site occupancies of 0.65 and 0.35 for the major and minor
72 components of disorder respectively. Crystal data, data collection and refinement parameters are
73 given in Table 3. Selected bond parameters are given in Table 4. ORTEP diagrams of (1), (2) and
74 (3) are shown in Figures 1, 2 and 3 respectively.

75 2.2 Preparation of the complexes

76 2.2.1 Preparation of tris(cyclohexylmethyldithiocarbamato)bismuth(III); [Bi(chmdtc)₃](1)

77 N-cyclohexyl-N-methylamine (6 mmol; 0.78 mL) and carbon disulfide (6 mmol; 0.36 mL)
78 in ethanol were mixed under ice-cold condition (5°C) to obtain yellow dithiocarbamic acid solution.
79 To the freshly prepared dithiocarbamic acid solution, acidified solution of Bi(NO₃)₃ pentahydrate (2
80 mmol; 0.96 g) was added with constant stirring. A yellow solid separated from the solution, which
81 was filtered, washed with alcohol and was dried in air. (Yield: 73%, dec., 124°C. Anal. calc. for
82 C₂₄H₄₂BiN₃S₆ (774.0): C, 37.24; H, 5.47; N, 5.42. Found: C, 37.19; H, 5.42; N, 5.38 %)

83 2.2.2 Preparation of tris(cyclohexylethyldithiocarbamato)bismuth(III); [Bi(chedtc)₃](2)

84 N-cyclohexyl-N-ethylamine (0.03 mol, 4.49 mL), carbon disulfide (0.03 mol, 5 mL) in
85 methanol (20 mL) and a weakly acidified solution of bismuth(III) nitrate pentahydrate (0.01 mol,
86 4.85g) were used for the preparation. A similar procedure as described in 2.2.1 was used for the
87 preparation. (Yield: 78%, m.p., 188°C. Anal. calc. for $C_{55}H_{96}Bi_2Cl_4N_6S_{12}$ (1785.9): C, 36.99; H,
88 5.42; N, 4.70. Found: C, 36.95; H, 5.38; N, 4.66 %)

89 2.2.3 Preparation of tris(dicyclohexyldithiocarbamato)bismuth(III); $[Bi(dchdtc)_3]$ (**3**)

90 A similar procedure as described in 2.2.1 was employed for the preparation of the
91 dicyclohexylamine analogue. N,N-dicyclohexylamine (0.03 mol, 4.49 mL), carbon disulfide (0.03
92 mol, 5 mL in 20 mL methanol) and bismuth(III) nitrate pentahydrate (0.01 mol, 4.85g) were used
93 for the preparation. (Yield: 67%, m.p., 145°C. Anal. calc. for $C_{41}H_{69}BiN_4S_6$ (1019.3): C, 48.31; H,
94 6.82; N, 5.49. Found: C, 48.26; H, 6.78; N, 5.45 %)

95 2.2.4 Preparation of nano Bi_2S_3 by non-conventional solvothermal decomposition of 96 Tris(disubstituteddithiocarbamato)bismuth(III)

97 1mM of tris(disubstituteddithiocarbamato)bismuth(III) complexes (**1**), (**2**) and (**3**) as clear
98 solutions in chloroform (100 mL) were heated with diethylenetriamine (2 mL) at 60°C for 45
99 minutes. Solid yellow bismuth sulfide obtained was separated from chloroform, washed with ether,
100 chloroform and dried in air.

101 3. Results and discussion

102 3.1 Infrared spectral studies

103 For complexes (**1**), (**2**) and (**3**) the ν_{C-N} (thioureide) bands are observed at 1474, 1467 and
104 1443 cm^{-1} respectively. The $\nu_{(C-S)}$ stretching bands are observed around 1000 cm^{-1} supporting [17]
105 the bidentate coordination mode of the dithiocarbamate to the metal center, and the ν_{C-H} bands are
106 observed in the range: 2850-2929 cm^{-1} .

107 3.2 *Electronic spectra*

108 Electronic spectra of the compounds show bands between 364 and 376 nm for the three
109 compounds which are due to intraligand π - π^* transitions, mainly associated with the N=C=S and
110 S=C=S groups [18, 19]. The electronic spectra of the complexes show charge transfer transitions in
111 the range: 410-423 nm.

112 3.3 *NMR spectral studies*

113 Chemical shifts reported in Spectral Data Base for Organic compounds (SDBS) for the
114 parent amines are shown in brackets in the Table 2 [20]. ^1H NMR of complex (1) shows an intense
115 signal at 5.08 ppm (2.303 ppm) corresponding to single proton integration due to α -CH of the
116 cyclohexyl ring. CH_3 protons (α' - CH_3) attached to the nitrogen appear at 3.28(s) ppm (2.421 ppm)
117 with proton integration corresponding to three. The α -CH and α' - CH_3 protons are affected to a
118 maximum extent on complexation. In the cyclohexyl ring all the equatorial protons are deshielded
119 to a large extent compared to the axial protons. The equatorial protons appear in the range: 1.80-
120 1.88 ppm. The axial protons appear between 1.69-1.71 ppm. ^{13}C NMR spectrum of (1) shows a
121 weak signal at 200.7 ppm due to the thiouriede carbon [21]. The α -carbon of cyclohexyl ring
122 appears at 62.8 ppm (58.63 ppm) and α' - CH_3 appears at 35.2 ppm (33.60 ppm). The β , γ - and δ -
123 carbon signals were the least affected and appeared at 25.40, 25.50 and 29.80 ppm respectively.

124 In complex (2), ^1H NMR of α -CH proton of the cyclohexyl ring appeared at 5.04 ppm and
125 α' - CH_2 appeared at 3.74-3.80 ppm corresponding to two protons. β' - CH_3 protons of the ethyl group
126 appeared as a well resolved triplet 1.50-1.95 ppm. ^{13}C NMR spectrum of (2) showed the
127 characteristic thiouriede signal at 200.6 ppm. β' - CH_3 appeared at 14.40 ppm as a much shielded
128 signal and α' - CH_2 appears to be highly deshielded at 43.60 ppm. α - CH signal of the cyclohexyl

129 ring appears at 63.20 ppm. The β,γ - and δ - carbon signals which were the least affected on
130 complexation appeared at 30.46 and between 24.60 to 25.70 ppm.

131 In the case of complex (**3**), α -CH proton of the cyclohexyl ring was observed at 5.31 ppm (2.546
132 ppm). β , γ - and δ -CH₂ signals appeared in the region of 1.82-2.09(e) ppm (collapsed) (1.606 - 1.856
133 ppm). The axial proton signals appeared between 1.35-1.53 ppm(1.021 - 1.246 ppm). ¹³C NMR
134 exhibited a weak characteristic signal due to thiouriede carbon at 200.8 ppm. ¹³C NMR signal
135 corresponding to the α -C(H) carbon of the cyclohexyl ring was found to be significantly shielded
136 and appeared at 65.21 ppm (53.17 ppm) . β -C(H₂), and γ -C(H₂) carbons appeared in the region of
137 25.03 - 29.78 ppm (26.32 – 34.51ppm). Signals observed at ~ 7.20 and 2.35 ppm in the ¹H NMR
138 spectra of the three compounds are due to the aromatic and methyl protons of toluene which is the
139 solvent used for crystallization. NMR spectra of the complexes clearly indicated that the immediate
140 environment around thiouriede nitrogen was largely affected by complex formation.

141 3.4 Thermogravimetric analysis

142 Thermal analyses of the compounds were carried out under nitrogen atmosphere. A toluene
143 recrystallized sample of (**1**) was used for the thermal analysis and hence a loss of solvent was
144 observed. [Bi(chmdtc)₃](**1**) showed initial loss of the solvent of crystallization, toluene around
145 198°C. A large mass loss (63.9%) was observed in the range of 260-320 °C. At temperatures above
146 500 °C, the mass loss was insignificant and the residue agreed well for Bi₂S₃ as the residue (Exptl.:
147 30.3%; Calcd.: 29.7%). [Bi(chedtc)₃](**2**) showed a minor loss due to the solvent of crystallization,
148 CCl₄ at 160°C. A large chunk of mass (60.1%) was lost in the temperature range: 220-280 °C. Above
149 500 °C, the mass remained constant and the final residue confirmed the formation of Bi₂S₃ (Exptl.:
150 28.5%; Calcd.: 28.8%). [Bi(dchdtc)₃](**3**) followed a similar pattern of decomposition. Loss of
151 solvent of crystallization, CH₃CN was observed at 240 °C. Largest mass loss (62.0%) was observed
152 in the temperature range: 250-290 °C. The final residue formed above 500 °C was Bi₂S₃ (Exptl.:
153 26.2%; Calcd.: 25.2%). Thermal analysis confirmed the proposed formulae of the compounds. The

154 most important observation is that in all the three compounds the final residue was found to be
155 Bi_2S_3 . Among the three compounds the dicyclo- analogue, $[\text{Bi}(\text{dchdtc})_3]$ (**3**) showed the highest
156 thermal stability.

157 3.5 Structural analysis

158 $[\text{Bi}(\text{chmdtc})_3]$ (**1**) crystallizes in monoclinic lattice with four molecules per unit cell. The
159 asymmetric unit of (**2**) contains two crystallographically independent $[\text{Bi}(\text{chedtc})_3]$ complex
160 molecules of similar conformation and one disordered CCl_4 solvent molecule of crystallization.
161 Complex (**3**) crystallizes with acetonitrile solvent molecules in a stoichiometric complex/solvent
162 molar ratio of 1:1. The dithiocarbamate group in all complexes acts in the usual asymmetric
163 bidentate mode, each ligand chelating Bi through a shorter (mean value 2.72(3) Å) and a
164 longer (mean value 2.88(2) Å) Bi–S bond. It is noticeable that in the ligands the C–S bonds
165 associated with the shorter Bi–S bonds are significantly longer (mean value 1.734(4) Å) than
166 those associated with the longer Bi–S bonds (mean value 1.717(4) Å). The thioureide C–N
167 distances (mean value 1.332(3) Å for all complexes) indicate a delocalization of the electron
168 density over the S_2CN fragment and suggest a partial double bond character of these bonds. The
169 observed values of the Bi–S, C–S and C–N bonds are in good agreement with those calculated
170 for 13 related bismuth dithiocarbamate complexes reported in the literature recently [22, 23],
171 where the mean shorter and longer Bi–S distances are 2.719(14) and 2.889(6) Å, respectively,
172 the corresponding mean longer and shorter C–S distances are 1.728(3) and 1.709(3) Å,
173 respectively, and the mean value of the C–N bonds is 1.330(3) Å. The BiS_6 chromophore in
174 $[\text{Bi}(\text{mchdtc})_3]$ (**1**) assumes a remarkably distorted octahedral geometry, similar to that observed in
175 tris(N-(n-hexyl)-N-methyldithiocarbamate-S,S')bismuth(III) [24]. The best equatorial plane is
176 defined by the S1/S3/S4/S6 set of donor atoms (r.m.s. 0.0501; maximum deviation 0.0767(10) Å

177 for atom S4) and the apical positions occupied by atoms S2 and S5. The bismuth cation is displaced
178 from the equatorial plane by 0.58752(10) Å toward S5. The S–Bi–S bond angles fall in the range
179 61.55(3)–153.34(3)°. The coordination geometry for both [Bi(chedtc)₃] (**2**) and [Bi(dchdctc)₃] (**3**)
180 should be better described as distorted pentagonal pyramidal instead, as usually observed in most
181 related bismuth dithiocarbamate complexes. The basal plane is defined by atoms S1/S2/S3/S5/S6
182 (r.m.s 0.4141; maximum displacement 0.605(2) Å for atom S2) and S7/S8/S9/S10/S11 (r.m.s.
183 0.2883; maximum displacement 0.466(3) Å for atom S9) in (**2**), and by atoms S1/S2/S3/S4/S6
184 (r.m.s. 0.1891; maximum displacement 0.3072(9) Å for atom S4) in (**3**). Atoms S4 and S12 in (**2**)
185 and S5 in (**3**) occupy the vertices and are displaced by 2.2479(1), 2.2610(16) and 2.0983(7) Å,
186 respectively, from the least square mean basal plane. The bismuth centres protrude from the
187 respective mean basal plane in opposite direction to the apical position by 0.3024(2) and
188 0.2789(2) Å in (**2**) and 0.43876(11) Å in (**3**). The S–Bi–S bond angles are not dissimilar to
189 those found in (**1**) ranging from 62.25(5) to 158.22(5)° in (**2**) and from 61.89(6) to 159.97(6)° in
190 (**3**). The different coordination geometry observed in [Bi(chmdtc)₃] (**1**) may be attributed to the
191 steric demand of the methyl substituent of the carbamate groups which is comparatively less
192 demanding than that of the ethyl and cyclohexyl analogues and hence the six coordinated
193 bismuth distorts to a lesser extent from the preferred octahedral geometry.

194 All complexes form dimeric units through non-covalent Bi⋯S interactions involving
195 symmetry related molecules as depicted in Figure 4, with Bi⋯S distances (3.2375(10) Å in (**1**);
196 3.3587(17) and 3.1449(15) Å in (**2**); 3.3260(6) Å in (**3**) notably shorter than the sum of the van
197 der Waals radii (1.80 for S [25] and 2.07 for Bi [26]). The Bi⋯Bi separations within the dimers
198 are 4.9110(5), 4.4655(4)-4.8894(4) and 4.5058(3) Å in (**1**), (**2**) and (**3**), respectively. The
199 molecular conformation of the complexes is stabilized by intramolecular C–H⋯S hydrogen

200 bonds involving methine and methylene hydrogen atoms of the ligands with H...S distances
201 varying in the range 2.44–2.46 Å in **(1)**, 2.44–2.46 Å in **(2)** and 2.39–2.76 Å in **(3)**.

202 3.6 Continuous shape measure

203 Continuous Shape measure (CShM) effectively quantifies the distance of a given structure
204 from the desired ideal symmetry or from a reference shape [27-30]. In practice, idealizations of
205 molecular structures is achieved by associating the position of a set of atoms with the vertices of a
206 reference polyhedron and qualitative descriptions such as ‘slightly distorted’ or ‘severely distorted’
207 relative to the reference polyhedron are often required. To quantify the degree of distortion of a
208 particular molecular structure from an ideal polyhedron one can use symmetry measures.

209 Continuous shape measure (CShM) methodology has been successfully applied to transition metal
210 complexes and metal oxides. For six coordination, the ideal geometries are ideal octahedron (iOh)
211 or ideal trigonal prism (itp). In the present investigation, the coordination around bismuth in **(2)** and
212 **(3)** is distorted pentagonal pyramid whereas in **(1)** it’s a distorted octahedron. It is natural to
213 consider the transformation of ppy to iOh or itp. In the present case, the Continuous Shape measure
214 calculations on the three complexes for the BiS₆ core yielded 10.237607, 27.662944 and 29.921790
215 for **(1)**, **(2)** and **(3)** respectively. The observed CShM values follow the order for **(3)** > **(2)** > **(1)**.

216 Complex **(3)** deviates to the largest extent from the octahedral geometry than the other two because
217 of the largest steric demand of the two cyclohexyl rings. Between the two, the methyl analogue **(1)**
218 is closer to the octahedral geometry than its ethyl analogue **(2)**. The observed CShM value clearly
219 indicate the closeness of **(1)** to octahedral geometry. The other two BiS₆ cores associated with **(2)**
220 and **(3)** are not close to octahedral geometry but to pentagonal pyramid (ppy) geometry as evident
221 from S-Bi-S angles. Between the two, compound **(2)**, shows four of the five S-Bi-S angles in the
222 range of 87.34(5) to 93.63(6)^o indicating a distorted pentagonal pyramid. The axial Bi-S bonds are

223 shorter than the equatorial bonds in compounds (2) and (3). All the three complexes show little
224 tendency to distort towards trigonal prismatic geometry. Distortion from the octahedral geometry to
225 pentagonal pyramid is minimal in the methyl analogue and is a maximum in the dicyclohexyl
226 analogue due to steric demands which is quantified by the reported values.

227 3.7 BVS calculations

228 Bond valence sum (BVS) calculations offer a reliable method of assigning formal oxidation
229 states of an atom in a compound from the bond parameters. The method depends on the R_{ij} value
230 for an i-j bond in a compound which is predominantly ionic [31]. In a compound, the oxidation
231 state of a central atom 'i' bonded to 'j' corresponds to the bond valence, S_{ij} , and the total valence of
232 the central atom which is its oxidation state, $\sum S_{ij} = \exp[(R_o - R_{ij})/b]$ and R_o is used as
233 reported[32,33] and R_{ij} is the experimentally determined bond distance. The constant b can be
234 assumed to be 0.37[34, 35]. Bond valence sums calculated for the complexes from the structural
235 data reported for the compounds in this study are 3.2618, 3.2811 and 3.3833 for (1), (2) and (3)
236 respectively. The calculated values have been found to be higher than the expected formal oxidation
237 state of +3. The higher values observed in the present set of compounds support the fact that the Bi-
238 S bonds are more covalent.

239 3.8 Characterization of Bi_2S_3

240 3.8.1 Powder XRD

241 Powder XRD of the solvothermally prepared bismuth sulfide is shown in Figure 5 along
242 with SEM and EDX. The broadened PXRD indicates the *nano* sized nature of the sample and
243 matched well with the JCPDS pattern reported for Bi_2S_3 , PDF # 75-1306 and two strong signals
244 corresponding to 26.76° (130), 29.93° (211) are observed[36,37]. On heating the three compounds
245 under identical conditions in diethylenetriamine at 60°C , Bi_2S_3 appeared as a precipitate very early

246 in the case of (3) compared to other two compounds within the shortest period compared to the
247 other two. Hence qualitatively, the ease of formation of the nanosulfide from the dithiocarbamates
248 based on its first appearance from (3) was slightly better than from the compounds (1) and (2).
249 Based on the observation, the ease of formation of nanosulfide from the bismuth dthiocarbamates
250 follows the order: (3) > (1) > (2). However, the mean Bi-S bond distances for the three compounds
251 are almost similar (2.8125(10), 2.8129(17) 2.7977(9) Å in (1), (2) and (3) respectively).

252 3.8.2 SEM-EDX

253 SE micrographs of the prepared bismuth sulfide are shown in Figures 5. The morphology of
254 surface shows crystalline grains with large size distribution. The energy dispersive spectrum
255 confirmed the presence of bismuth and sulfur in 2:3 ratio.

256 3.8.3 HRTEM and SAED

257 HRTEM and SAED (inset) are shown in Figure 6. HRTEM showed the Bi₂S₃ to be *nano*
258 wires < 10 nm size. SAED pattern confirmed the crystalline nature of the sample. Fringe spacing of
259 the Bi₂S₃ wires is ~ 0.5nm. The SAED pattern showed strong diffractions due to (001) and (120)
260 oriented single crystals.

261 4. Conclusions

262 [Bi(chmdtc)₃] (1), [Bi(chedtc)₃] (2) and [Bi(dchdte)₃] (3) show interesting variations
263 in the geometry around bismuth. The single crystal X-ray structures showed the Bi-S bonds to vary
264 largely due to variations in the steric effects. NMR spectra of the complexes clearly indicated that
265 the immediate environment around thiouriede nitrogen was largely affected by complex formation.
266 CShM calculations on the chromophores clearly quantify the extent of deviation from the ideal
267 octahedral geometry. BiS₆ chromophore in (1) is a distorted octahedron whereas in the other two,

268 distorted pentagonal pyramidal geometry prevails. Stabilization of the dimer in (2) is favoured to a
269 large extent than the other two because of the pentagonal pyramid geometry assumed by the BiS₆
270 core. In the three compounds, the steric effect is active in controlling the geometry around bismuth.
271 The bond valence sums indicate the highly covalent nature of the Bi-S bonds. Non conventional
272 solvothermal decomposition of the compounds yield *nano* Bi₂S₃. The ease of formation of the
273 nanosulfide followed the order: (3) > (1) > (2). The *nano* wires of Bi₂S₃ have been characterized by
274 a host of techniques.

275 **Appendix A**

276 **Supplementary material**

277 CCDC **967477**, **954122** and **954123** contain the supplementary crystallographic data for (1), (2) and
278 (3). These data can be obtained free of charge from The Cambridge Crystallographic
279 Data Centre via www.ccdc.cam.ac.uk/data_request/cif.

280

281

282

283

284

285

286

287

288

289

290

291 **References**

- 292 [1] L. Martinez, A. Stavrinadis, S. Higuchi, S. L. Diedenhofen, M. Bernechea, K. Tajima, G.
293 Konstantatos, *Phys.Chem. Chem. Phys.*, 15 (2013) 5482-5487.
294
- 295 [2] (a) L. Martinez, M. Bernechea, F. P. G. de Arquer, G. Konstantatos, *Adv. Energy Mater.*
296 1 (2011) 1029–1035.
297 (b) Z. Wang, S. Qu, X. Zeng, J. Liu, F. Tan, L. Jin, Z. Wang, *Appl. Surf. Sci.* 257 (2010)
298 423–428.
299
- 300 [3] M. Alipour, C. Dorval, Z.E. Suntres, A. Omri, *J. Pharmacol.*, 63 (2011) 999-1007.
- 301
- 302 [4] Y. Fang, C. Peng, R. Guo, L. Zheng, J. Qin, B. Zhou, M. Shen, X. Lu, G. Zhang, X. Shi,
303 *Analyst*, 138 (2013) 3172-3180.
- 304 [5] (a) H. Li, C.S. Lai, J. Wu, P.C. Ho, D. de Vos, E.R.T. Tiekink, *J. Inorg. Biochem.*, 101
305 (2007) 809-816;
- 306 (b) H. P. S. Chauhan, N. M. Shaik, U. P. Singh, *Appl. Organometal. Chem.*, 20 (2006)
307 142-148;
- 308 (c) H. P. S. Chauhan, N. M. Shaik, U. P. Singh, *Appl. Organometal. Chem.*, 20 (2006)
309 1132-1139.
310
- 311 [6] I.I. Ozturk, C.N. Banti, N. Kourkoumelis, M.J. Manos, A.J. Tasiopoulos, A.M. Owczarzak,
312 M. Kubicki, S.K. Hadjikakou, *Polyhedron*, 67 (2014) 89-103.
313
- 314 [7] S.S. Garje, V.K. Jain, *Coord. Chem. Rev.*, 236 (2003) 35-56.
- 315 [8] G.G. Briand, N. Burford, *Chem. Rev.*, 99 (1999) 2601-2657.
- 316 [9] M.A. Malik, M. Afzaal, P. O'Brien, *Chem. Rev.*, 110 (2010) 4417-4416.
- 317 [10] A. Gupta, R.K. Sharma, R. Bohra, V.K. Jain, J.E. Drake, M.B. Hoursthouse, M.E. Light, J.
318 *Organomet. Chem.* 678 (2003) 122-127.
319
- 320 [11] C. L. Teske, W. Bensch, *Z. Anorg. Allg. Chem.*, 637 (2011) 406–414.
- 321 [12] Bruker AXS Inc., 6300 Enterprise Lane, Madison, WI 53719-1173, USA.
- 322 [13] N. Walker, D. Stuart, *Acta Crystallogr.*, A39 (1983) 158-166.

- 323 [14] P. Gluzinski, Set of Programs for X-ray Structural Calculation, Icho Polish Academy of
324 Sciences, Warsaw, Poland, 1987.
325
- 326 [15] G.M. Sheldrick, SHELX 97, Program for Crystal Structure refinement, University of
327 Gottingen, Germany, 1997.
328
- 329 [16] L.J. Farrugia, ORTEP-3 for Windows, University of Glasgow, Scotland, UK, 1999.
- 330 [17] B. Arul Prakasam, K. Ramalingam, G. Bocelli, A. Cantoni, Phosphorus Sulfur Silicon, 184
331 (2009) 2020-2028.
332
- 333 [18] R. Baskaran, K. Ramalingam, G. Bocelli, A. Cantoni, C. Rizzloi, J. Coord. Chem., 61
334 (2008) 1710-1719.
- 335 [19] M.V. Rajasekaran, G.V.R. Chandramouli, P.T. Manoharan, Chem. Phys. Lett., 162 (1989)
336 110-116.
- 337 [20] http://sdbs.riondb.aist.go.jp/sdbs/cgi-bin/cre_index.cgi
- 338 [21] H.L.M. Van Gaal, J.W. Diesveld, F.W. Pijpers, J.G.M. Van Der Linden, Inorg. Chem., 18
339 (1979) 3246-3251.
- 340 [22] (a) F. Li, H.D. Yin, J. Zhai, D.Q. Wang, Acta Crystallogr., E62 (2006) m1083-m1085.
341 (b) C. S. Lai, E. R. T. Tiekink, Z. Kristallogr., 222 (2007) 532-538.
342 (c) H.D. Yin, F. Li, D.Q. Wang, J. Coord. Chem., 60 (2007) 1133-1141.
343 (d) H.D. Yin, C.H. Wang, Appl. Organomet. Chem., 18 (2004) 420.
344 (e) V. Venkatachalam, K. Ramalingam, G. Bocelli, A. Cantoni, Inorg. Chim. Acta, 261
345 (1997) 23-28.
346
- 347 [23] (a) I. Baba, K. Karimah, Y. Farina, A. H. Othman, A. R. Ibrahim, A. Usman, H.K. Fun, S.
348 W. Ng, Acta Crystallogr., E56 (2002) m756-m757.
349 (b) R.Z. Sun, Y.C. Guo, W.M. Liu, S.Y. Chen, Y. Q. Feng, J. Huaxue, Chin. J.
350 Struct. Chem., 31 (2012) 655-660.
351 (c) K. Y. Low, I. Baba, Y. Farina, A. H. Othman, A. R. Ibrahim, H.K. Fun, S. W. Ng,
352 Main Group Met .Chem., 24 (2001) 451-452.

- 353 (d) F. Li, H.D. Yin, J. Zhai, D.Q. Wang, *Acta Crystallogr.*, E62 (2006) m2552-m2554.
354
- 355 [24] O. C. Monteiro, H. I. S. Nogueira, T. Trindade, M. Motevalli, *Chem. Mater.*, 13 (2001)
356 2103-2111.
- 357 [25] A. Bondi, *J. Phys. Chem.*, 68 (1964) 441-451.
- 358 [26] M. Mantina, A. C. Chamberlin, R. Valero, C. J. Cramer, D. G. Truhlar, *J. Phys. Chem., A*
359 113 (2009) 5806-5812.
- 360
- 361 [27] S. Alvarez, D. Avnir, M. Llunell, M. Pinsky, *New J. Chem.*, 26 (2002) 996-1009.
- 362 [28] H. Zabrodsky, S. Peleg, D. Avnir, *J. Am. Chem. Soc.*, 114 (1992) 7843-7851.
- 363 [29] K.M. Ok, P.S. Halasyamani, D. Casanova, M. Llunell, S. Alvarez, *Chem. Mater.*,
364 18 (2006) 3176-3183.
- 365 [30] S. Keinan, D. Avnir, *J. Am. Chem. Soc.*, 122 (2000) 4378-4384.
- 366 [31] N.E. Bresse, M. O'Keefe, *Acta Crystallogr., B*, 47 (1991) 192-197.
- 367 [32] S.P. Summers, K.A. Abboud, S.R. Farrah, G.J. Palenik, *Inorg. Chem.*, 33 (1994) 88-92.
- 368 [33] I.D. Brown, D. Altermatt, *Acta Crystallogr.*, B41 (1985) 244-247.
- 369 [34] I. D. Brown, *The Chemical Bond in Inorganic Chemistry*, Oxford University Press, Oxford,
370 UK, 2002.
- 371 [35] I. D. Brown, *Chem. Revs.*, 109 (2009) 6858-6919.
- 372 [36] K.R. Chaudhari, A.P. Wadawale, S. Ghoshal, S. M. Chopade, V.S. Sagoria, V.K. Jain,
373 *Polyhedron*, 362 (2009) 1819-1824.
- 374 [37] K.R. Chaudhari, N. Yadav, A. Wadawale, V.K. Jain, *Polyhedron*, 363 (2010) 375-380.

375

376

377

378 **Captions for figures**379 Figure 1. ORTEP of [Bi(chmdtc)₃] (**1**). Hydrogen atoms are omitted for clarity

380

381

382 Figure 2. ORTEP of one complex molecule in [Bi(chedtc)₃] (**2**). Only the major component
383 of the disordered ethyl chain is shown. Hydrogen atoms are omitted for clarity

384

385

386 Figure 3. ORTEP of [Bi(dchdte)₃] (**3**). Hydrogens atoms are omitted for clarity

387

388 Figure 4. ORTEP plot of the dimers

389

390

391

392 Figure 5 PXRD, SEM and EDX of *nano* Bi₂S₃393 Figure 6 HRTEM and SAED of *nano* Bi₂S₃

394

395

396

397

398

399

400

401

402

403

404

405

406

407

408

409

410 Table 1 Electronic and IR spectral data

411
412
413
414
415
416
417
418
419
420
421
422
423
424
425
426
427
428
429

Compound	Uv-Vis (nm)		IR (cm ⁻¹)			† Free
	CT	Intraligand	ν_{C-N}	† ν_{C-S}	ν_{C-H}	
[Bi(chmdtc) ₃] (1)	418	364	1474	1004 (1010)	2850-2925*	
[Bi(chedtc) ₃] (2)	420	367	1467	1009 (1017)	2852-2929*	
[Bi(dchdtc) ₃] (3)	423	376	1443	1010 (1018)	2851-2927*	

dithiocarbamate ν_{C-S} wave numbers are given in parentheses

* ν_{C-H} wave numbers for the free dithiocarbamates are in the range of 2850-2930 cm⁻¹

430

431 Table 2 NMR spectral data (ppm) †

Complex	NMR	α -CH	β -CH ₂ / γ -CH ₂ & δ -CH ₂	α' -CH ₃ /CH ₂	N ¹³ CS ₂
[Bi(chmdtc) ₃] (1)	¹ H	5.08 (2.303)	1.80-1.88(e) 1.69-1.71	3.28 (2.421)	-
	¹³ C	62.8 (58.63)	29.80 25.40,25.50	35.2 (33.60)	200.7
[Bi(chedtc) ₃] (2)	¹ H	5.04	1.83-1.93(e) 1.56-1.69	3.74-3.80 1.31-1.37	-
	¹³ C	63.2	30.46 24.60-25.70	43.60 14.40	200.6
[Bi(dchdtc) ₃] (3)	¹ H	5.31 (2.546)	1.82-2.09(e) (1.606 - 1.856) 1.35-1.53 (1.021 - 1.246) (Collapsed)	-	-
	¹³ C	65.21 (53.17)	29.66 25.03 - 29.78 (26.32 - 34.51)	-	200.8

432

433 † Chemical shifts reported in Spectral Data Base for Organic compounds (SDBS) for the parent amines are
434 shown in brackets

435

436

437 Table 3. Crystal data, data collection and refinement parameters for
 438 [Bi(chmdtc)₃], [Bi(chedtc)₃] and [Bi(dchdtc)₃]

Complex	[Bi(chmdtc) ₃]	[Bi(chedtc) ₃]	[Bi(dchdtc) ₃]
Empirical formula	C ₂₄ H ₄₂ BiN ₃ S ₆	2(C ₂₇ H ₄₈ BiN ₃ S ₆)·CCL ₄	C ₃₉ H ₆₆ BiN ₃ S ₆ ·C ₂ H ₃ N
Formula weight	774.0	3571.96	1019.34
Colour	Yellow	Yellow	Yellow
Habit	Block	Block	Prism
Crystal system	Monoclinic	Monoclinic	Monoclinic
Space group	P 2 ₁ /c	C 2/c	P 2 ₁ /c
Crystal dimension(mm ³)	0.32 × 0.24 × 0.18	0.28 × 0.27 × 0.24	0.27 × 0.23 × 0.18
a (Å)	12.6224(17)	30.3139(17)	10.5705(8)
b(Å)	20.526(3)	14.9828(8)	16.1324(12)
c(Å)	13.1879(17)	34.549(3)	27.975(2)
α (°)	90.00	90.00	90.00
β (°)	109.137(2)	108.3958(12)	97.9920(12)
γ (°)	90.00	90.00	90.00
U (Å ³)	3228.0(8)	14889.8(17)	4724.2(6)
Z	4	4	4
Dc(g cm ⁻³)	1.593	1.593	1.433
F(000)	3228.0(8)	7152	2088
λ(Å)	MoKα (0.71073)	MoKα (0.71073)	MoKα (0.71073)
θ range (°)	1.42-25.25	1.42-25.25	1.46-25.50
Scan type	ω scan	ω scan	ω scan
Index range	-15 ≤ h ≤ 15; -25 ≤ k ≤ 25; -16 ≤ l ≤ 16	-36 ≤ h ≤ 36; -17 ≤ k ≤ 17; -41 ≤ l ≤ 41	-12 ≤ h ≤ 12; -19 ≤ k ≤ 19; -33 ≤ l ≤ 33
Reflections collected	6350	13477	8789
Reflections [Fo > 2 σ (Fo)]	4885	9374	7644
Weighting scheme	w = 1/[Σ(Fo ²) + (0.0212p) ²] where P = (Fo ² + 2Fc ²)/3	w=1/[s ² (Fo ²)+(0.0405P) ² +46 .8561P] where P=(Fo ² +2Fc ²)/3	w=1/[s ² (Fo ²)+(0.0218P) ² +2.2017P] where P=(Fo ² +2Fc ²)/3
Number of parameters refined	307	743	470
Final R, Rw (obs, data)	0.0206, 0.0432	0.0391, 0.0872	0.0210, 0.0485
GOOF	0.995	1.011	1.029

439

440

441

442

Table 4 Selected bond distances (Å) and bond angles (°)

443

[Bi(chmdtc) ₃]		[Bi(chedtc) ₃]			[Bi(dchdte) ₃]		
Bi1–S1	2.7770(9)	Bi1–S1	2.7554(17)	Bi2–S7	2.951(2)	Bi1–S1	2.9201(6)
Bi1–S2	2.6884(8)	Bi1–S2	2.8545(18)	Bi2–S8	2.8167(19)	Bi1–S2	2.8288(10)
Bi1–S3	2.9974(10)	Bi1–S3	2.9428(18)	Bi2–S9	2.776(2)	Bi1–S3	2.8359(8)
Bi1–S4	2.7876(10)	Bi1–S4	2.6060(18)	Bi2–S10	2.816(2)	Bi1–S4	2.8057(9)
Bi1–S5	2.9326(9)	Bi1–S5	2.9560(18)	Bi2–S11	2.8396(19)	Bi1–S5	2.5841(8)
Bi1–S6	2.6921(11)	Bi1–S6	2.7669(17)	Bi2–S12	2.6400(16)	Bi1–S6	2.8121(8)
C1–S1	1.721(3)	C1–S1	1.733(6)	C28–S7	1.731(6)	C1–S1	1.736(3)
C1–S2	1.729(3)	C1–S2	1.709(6)	C28–S8	1.714(7)	C1–S2	1.717(3)
C9–S3	1.706(3)	C10–S3	1.705(6)	C37–S9	1.719(9)	C14–S3	1.730(3)
C9–S4	1.739(4)	C10–S4	1.743(6)	C37–S10	1.719(8)	C14–S4	1.711(3)
C17–S5	1.702(3)	C19–S5	1.717(6)	C46–S11	1.703(6)	C27–S5	1.751(2)
C17–S6	1.742(3)	C19–S6	1.728(6)	C46–S12	1.743(6)	C27–S6	1.709(3)
N1–C1	1.329(3)	N1–C1	1.329(8)	N4–C28	1.330(9)	N1–C1	1.333(4)
N2–C9	1.337(4)	N2–C10	1.323(8)	N5–C37	1.334(11)	N2–C15	1.484(4)
N3–C17	1.331(4)	N3–C19	1.335(8)	N6–C46	1.327(8)	N3–C27	1.330(3)
S1–Bi1–S3	112.39(3)	S1–Bi1–S2	63.45(6)	S7–Bi2–S8	61.89(6)	S1–Bi1–S2	61.46(2)
S1–Bi1–S4	153.34(3)	S1–Bi1–S4	90.52(5)	S7–Bi2–S11	78.20(5)	S1–Bi1–S5	84.99(2)
S1–Bi1–S6	94.00(3)	S1–Bi1–S6	75.84(5)	S7–Bi2–S12	82.49(5)	S1–Bi1–S6	82.11(2)
S3–Bi1–S4	61.55(3)	S2–Bi1–S3	77.28(5)	S8–Bi2–S9	75.35(6)	S2–Bi1–S3	73.62(2)
S3–Bi1–S6	140.36(3)	S2–Bi1–S4	91.31(7)	S8–Bi2–S12	97.79(5)	S2–Bi1–S5	91.49(2)
S4–Bi1–S6	81.44(3)	S3–Bi1–S4	64.24(5)	S9–Bi2–S10	63.94(7)	S3–Bi1–S4	62.71(2)
S2–Bi1–S5	136.50(3)	S3–Bi1–S5	85.82(5)	S9–Bi2–S12	87.56(7)	S3–Bi1–S5	83.53(2)
		S4–Bi1–S5	93.63(6)	S10–Bi2–S11	81.83(6)	S4–Bi1–S5	81.95(2)
		S4–Bi1–S6	87.35(5)	S10–Bi2–S12	90.66(6)	S4–Bi1–S6	76.42(3)
		S5–Bi1–S6	62.25(5)	S11–Bi2–S12	65.56(5)	S5–Bi1–S6	66.09(2)

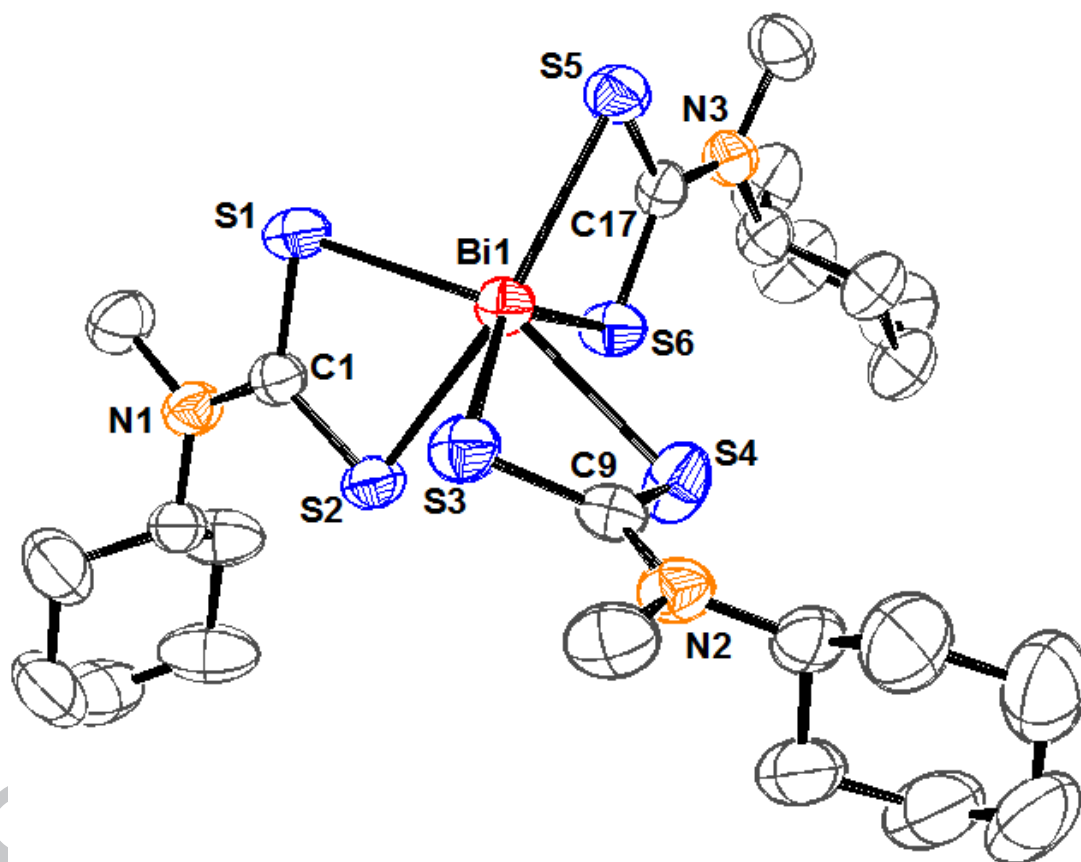
444

445

446

447

448



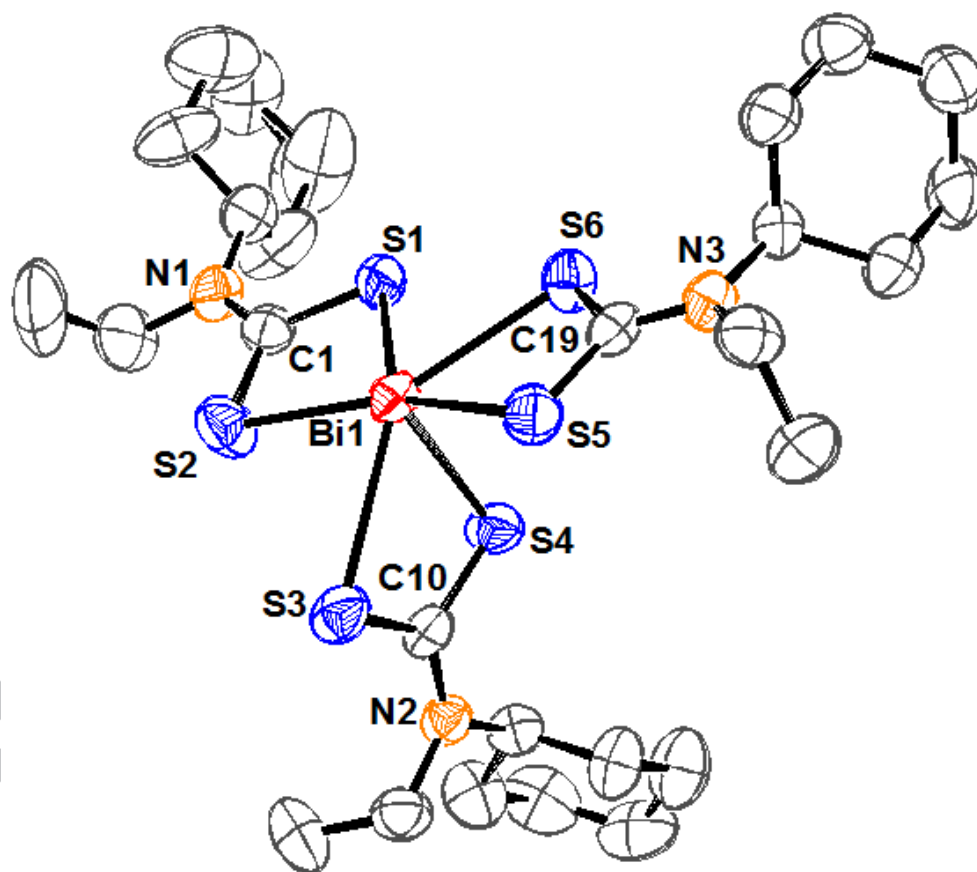
449

450

451

452

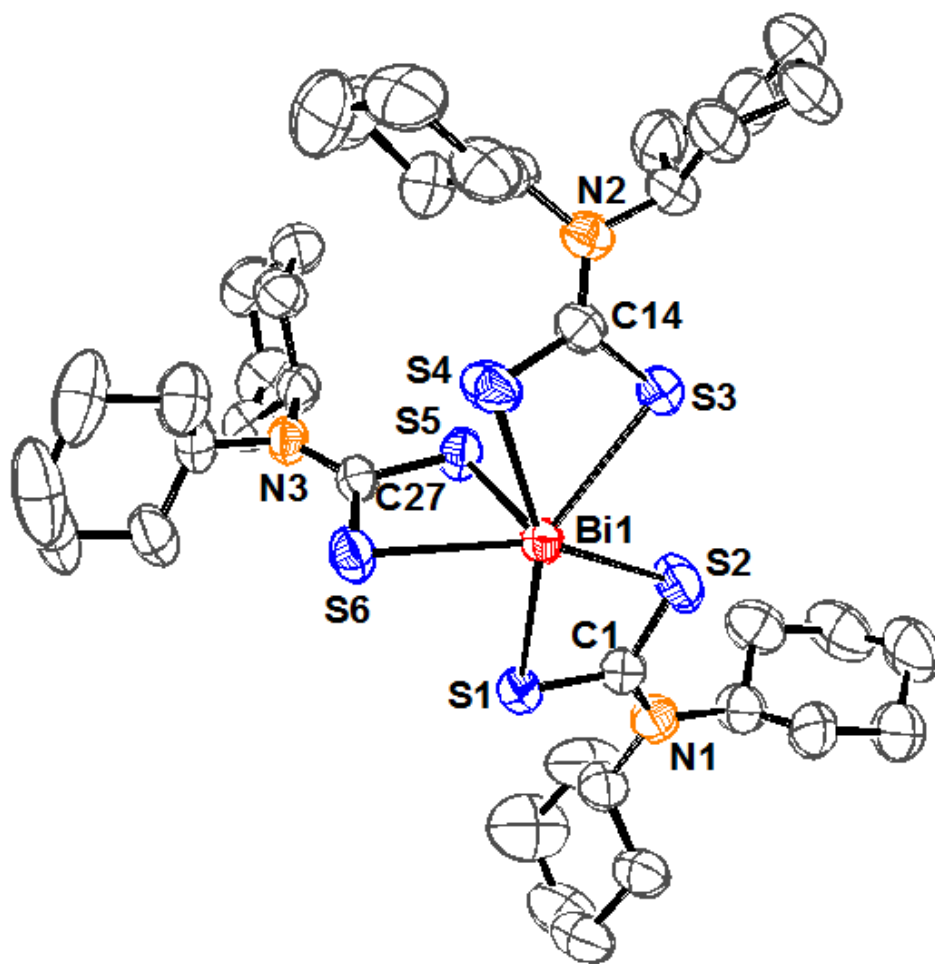
453
454
455
456
457
458
459
460



461

462
463
464
465
466

467
468
469
470
471
472
473
474
475
476
477



478

479

480

481

482

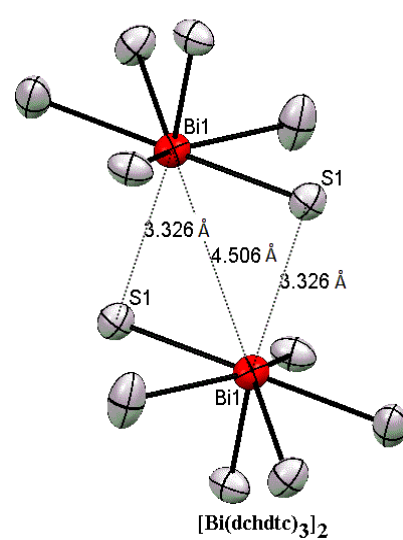
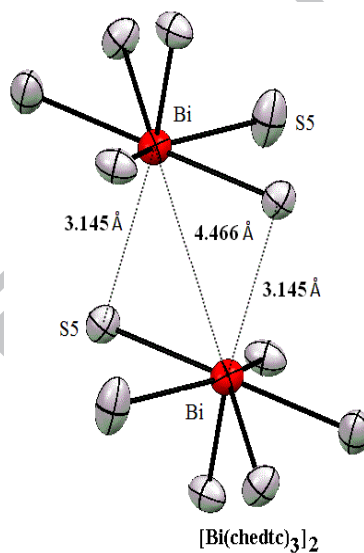
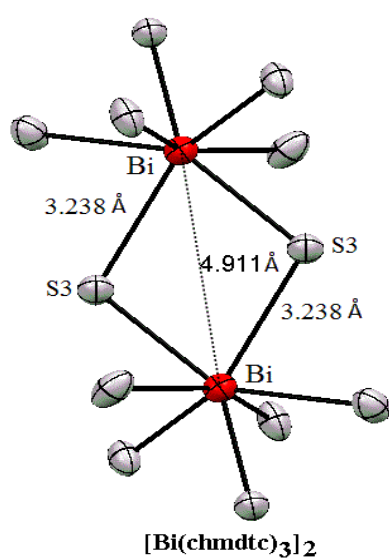
483

484

485

486

487



488

489

490

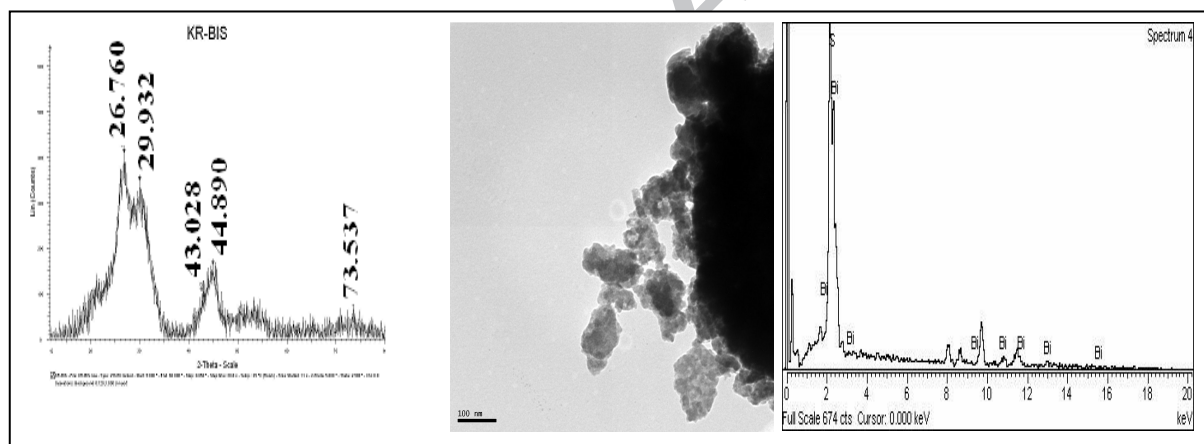
491

492

493

494

495
496
497
498
499
500
501
502
503
504
505
506
507
508
509
510
511
512
513
514
515
516
517



518

519

520

521

522

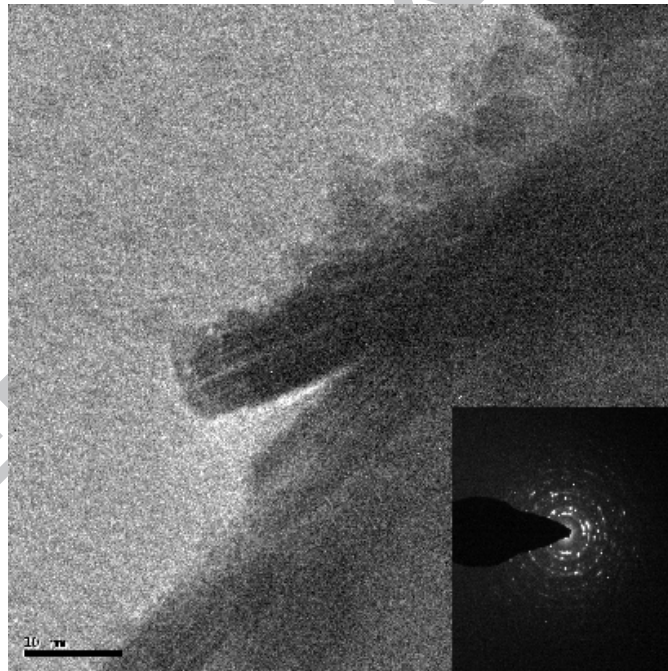
523

524

525

526

527



528

529

530

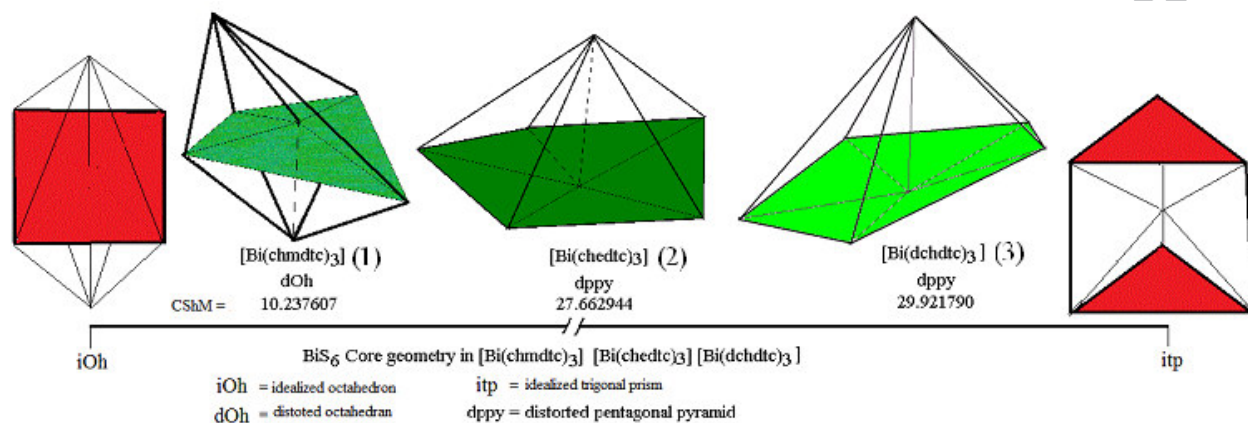
531 Synthesis, Structural, Continuous shape measure and Bond valence sum characterization of
532 bismuth(III) complexes of substituted dithiocarbamates and their solvothermal decomposition
533 **Subbarayan Sivasekar, Kuppukkannu Ramalingam,* Corrado Rizzoli and Nagarajan Alexander**

534 Geometrical distortions from iOh in tris(dithiocarbamato)bismuth(III) have been quantified by Continuous
535 Shape Measure (CShM) analysis. BiS_6 chromophore in $[Bi(chmdtc)_3]$ (**1**) is a distorted octahedron. The coordination
536 geometry in $[Bi(chedtc)_3]$ (**2**) and $[Bi(dchdc)_3]$ (**3**) should be described as distorted pentagonal pyramid. The higher
537 BVS values observed in the present set of compounds support the fact that the Bi-S bonds are more covalent.

538

539
 540 Synthesis, structural, Continuous shape measure and Bond valence sum characterization of
 541 bismuth(III) complexes of substituted dithiocarbamates and their solvothermal decomposition

542 Subbarayan Sivasekar, Kuppukkannu Ramalingam,* Corrado Rizzoli and Nagarajan Alexander



543

544

545

Highlights

- 546 ➤ Complete characterization of three bismuth - dithio complexes
- 547 ➤ Three well refined single crystal X-ray structures
- 548 ➤ The CShM evaluation correlated to distortion in geometry
- 549 ➤ Bond Valence Sums confirm the trivalent nature of bismuth
- 550 ➤ Nano bismuth sulfide characterized by PXRD, SEM, EDX and HRTEM

551

ACCEPTED MANUSCRIPT